

Classical Bouc-Wen hysteresis modeling and force control of a piezoelectric robotic hand manipulating deformable object

Supplementary material

Gerardo Flores, *Member, IEEE*, and Micky Rakotondrabe, *Member, IEEE*

SIMULATION RESULTS

For the simulation experiment, we chose the following system parameters: $\alpha_2 = 0.001[s]$, $\alpha_1 = 1$, $c_{ob} = 1[mNs/\mu m]$, $k_{ob} = 0.2675[mN/\mu m]$, $p = 1.3[\mu m/mN]$, $d_p = 1.0773[\mu m/V]$, $A_{bw} = 0.40648$, $B_{bw} = 0.40648$, and $\Gamma_{bw} = 0.00833$. The observer's parameters are $\theta = 8.8$, $k_o = 66.5945$, and $l_o = 10.2$. The control parameters are $k_1 = 120$, $k_2 = 100$, $M_1 = 7.1$, $L_1 = 7$, $M_2 = 16$, $L_2 = 15$, and $l = 0.65$. For the saturation function, we use a smooth function given by,

$$\sigma_i(s) = \begin{cases} \frac{\arctan(c_i[s-L_i])}{c_i} + L_i & \text{if } s > L_i \\ s & \text{if } |s| \leq L_i \\ \frac{\arctan(c_i[s+L_i])}{c_i} - L_i & \text{if } s < -L_i \end{cases} \quad (1)$$

where $c_i := \frac{\pi}{2(M_i - L_i)}$, with $M_i > L_i > 0$ for $i = \{1, 2\}$.

The system's initial conditions are $f(0) = 1.5[mN]$, $h(0) = 2$. While the initial conditions of the observer are all zero. The desired trajectory is given by [1],

$$\text{sqd}_c(t, \omega, \kappa) = \frac{\cos(\omega t)}{\sqrt{\kappa^2 \sin^2(\omega t) + \cos^2(\omega t)}} + 1; \quad (2)$$

with $\omega = 1$, $\kappa = 0.09$.

The force and hysteresis estimate with the proposed observer (19) are depicted in Fig. 1.

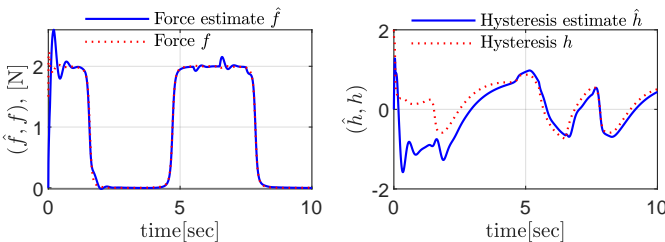


Fig. 1: Force and hysteresis estimates with the proposed observer. The convergence can be enhanced by conducting fine-tuning of the observer gains.

The force and its desired trajectory are depicted in Fig. 2, where disturbance $\delta(t)$ is also shown. The disturbance is

particularly severe at $t = 6$, but due to the accurate estimation of the disturbance, the controller's output feedback component can handle it effectively.

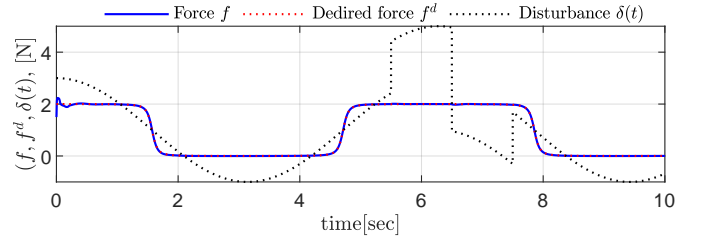


Fig. 2: The force f and the desired trajectory $f^d(t)$, and the disturbance $\delta(t)$. Notice how $\delta(t)$ is highly aggressive in $t \in [5.5, 6.5]$.

One of the primary objectives of control is to ensure that the tracking error remains within a predetermined set. This is demonstrated in Fig. 3, where we can observe that the conditions of Assumption 4 are met. The error trajectory never exceeds the threshold marked in magenta at $l = 0.5$. By choosing appropriate initial conditions for the error and/or desired trajectory described in Assumption 4, we can further decrease this threshold.

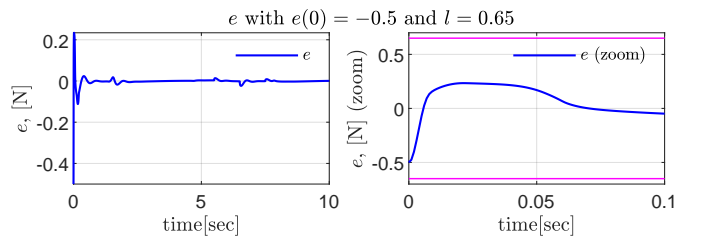


Fig. 3: The tracking error e and zoom of it. Notice that the e is always enclosed in the set $|e| < l$; the parameter l (and $-l$) appears magenta. The minor variations around $t = 6$ occur during the aggressive disturbance $\delta(t)$; please see Fig. 2.

Fig. 4 displays the proposed controller, the disturbance, and its estimate. Notably, the disturbance estimate initially exhibits an aggressive response, a normal occurrence due to the high-gain observer. The barrier term, represented by

$-\sigma_2\left(\frac{k_2 e}{l^2 - e^2}\right)$, is responsible for aggressively rejecting any error that approaches l , whereas the proportional term, denoted by $-\sigma_1([l^2 - e^2][k_1 e])$, is more effective for errors near the origin. This is depicted in the example of Fig. 5. Conversely, the smooth saturation functions $-\sigma_i(\cdot)$ serve the dual purpose of preventing spikes in the controller and allowing for the selection of high control gains. We have included a depiction of the argument of saturation functions $-\sigma_i(\cdot)$ in both cases, with and without saturation; see Fig. 4. It is important to note that as the error term e approaches the value of l , the magnitude of the argument in the control term $-\sigma_2(\cdot)$ increases exponentially. Therefore, saturation functions become necessary to prevent this exponential response.

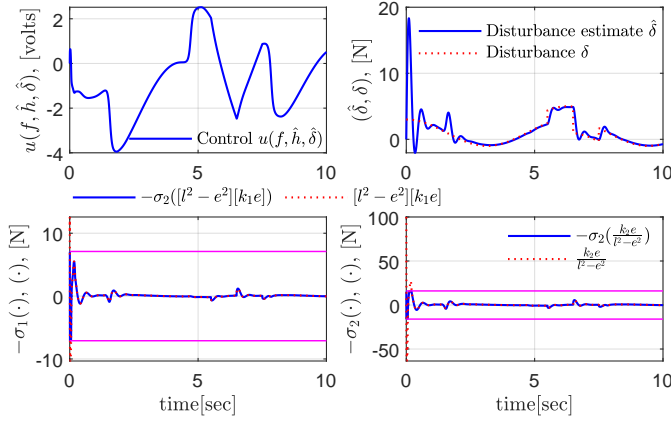


Fig. 4: Output feedback Barrier-Lyapunov-function and saturation-based controller, disturbance and its estimate, and the saturation terms of control (43). The saturation limits M_1 and M_2 are in magenta. To show the effect of the saturation control, we plot the arguments of saturation functions $-\sigma_1(\cdot)$ and $-\sigma_2(\cdot)$. Notice how the proposed control u maintains considerable limits and responds robustly against disturbances. This is due to the effect of saturation functions and the barrier term $k_2 e / (l^2 - e^2)$.

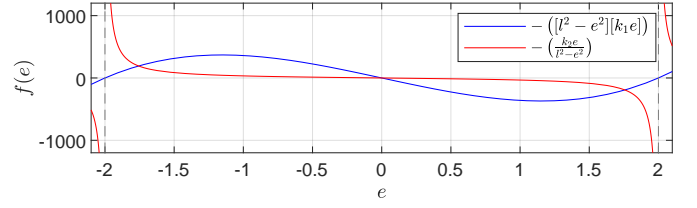


Fig. 5: This figure demonstrates the effectiveness of the proportional term (blue line) for errors close to the origin and the power of the barrier control term (red line) near the value of l , where, in this particular case, $l = 2$.

REFERENCES

- [1] M. Fern-Guasti, "Squdel Function: Square Wave Approximation Without Ringing," *Circuits, Systems, and Signal Processing*, vol. 38, no. 2, pp. 764–773, Feb. 2019.